This is the accepted manuscript made available via CHORUS. The article has been published as:

Controlling orbital magnetism of band electron systems via bath engineering

Subrata Chakraborty and So Takei

Phys. Rev. B **110**, L140405 — Published 10 October 2024

DOI: 10.1103/PhysRevB.110.L140405

Controlling Orbital Magnetism of Band Electron Systems via Bath Engineering

Subrata Chakraborty[1, 2, *] and So Takei[2, 3, †]

[1]*Fachbereich Physik, Universität Konstanz, D-78457 Konstanz, Germany*
[2]*Department of Physics, Queens College of the City University of New York, Queens, NY 11367, USA*
[3]*Physics Doctoral Program, Graduate Center of the City University of New York, New York, NY 10016, USA*

(Dated: September 3, 2024)

Orbital magnetism arises due to the coherent cyclotron motion of band electrons. System-bath entanglement is expected to disrupt this coherent electronic motion and quench orbital magnetism. Here, we show that a suitably-tailored bath can lead to an enhancement of the orbital diamagnetic susceptibility of a multi-band electron system and can even convert an orbital paramagnetic response into a diamagnetic one as the system-bath coupling is increased. We also demonstrate how a van Hove singularity in the bath density of states can be exploited to generate a giant enhancement of the orbital magnetic susceptibility. Our work opens doors to the possibility of controlling the orbital magnetic response of band electron systems through bath engineering.

Introduction.–The study of orbital magnetism in isolated band systems began nearly a century ago with the Landau-Peierls theory of diamagnetism in single-band systems [1, 2]. For multi-band systems, orbital magnetism can be non-trivial due to field-mediated couplings between different Bloch bands. Wallace and McClure first predicted that such inter-band effects can lead to anomalously large diamagnetism in graphene at the charge-neutrality point [3, 4]. Inter-band effects were later found to give divergent paramagnetism in two-dimensional (2D) band systems when the Fermi level is tuned to a van Hove singularity in the density of states [5]. Fukuyama first derived a useful expression for the orbital magnetic susceptibility of a multi-band system in terms of the electron Green function (GF) [6–8]. His works were further developed by others [9–11] to provide a systematic tool for computing the susceptibility of multi-band systems. Enhanced diamagnetism has been observed in Dirac materials, such as graphene and bismuth, when the chemical potential is tuned within the weak effective mass gap [11–15]. Strong orbital magnetism has also been reported in BiTeI semiconductor, where giant Rashba spin-orbit interaction mediates coupling between the valence and conduction bands [16–18].

While the orbital magnetism of isolated band systems is now well-studied, the same cannot be said for electrons coupled to a dissipative bath. Recent interests in the enhanced diamagnetism of isolated materials therefore lead us to question whether the orbital magnetic response of a multi-band system can be controlled by bath engineering. Orbital magnetism is precluded within classical statistical mechanics by the Bohr-van Leeuwen theorem [19–21]: Studies based on the quantum Langevin equation [22–24] have indeed shown that a vanishing diamagnetic moment is obtained in the limit of very strong energy-independent dissipation [25–30]. While dissipation, at first sight, seems to be harmful to diamagnetism, the circumstances under which it can be beneficial are counterintuitive and have not yet been identified. The goal of this work is to show how the orbital magnetic response of a multi-band system can be controlled and enhanced by opening the system to a bath with a suitably-tailored local density of states (LDOS).

* Correspondence to: schrkmv@gmail.com
† Correspondence to:stakei@qc.cuny.edu

In this work, we explore how the orbital magnetic susceptibility of a 2D band electron system can be controlled by entangling the system with a fermionic bath. Using the gauge-invariant Keldysh GF formalism, we derive an expression for the susceptibility that is valid for any band structure and arbitrary bath LDOS: This work therefore generalizes the GF expression for the susceptibility of an isolated system — see, e.g., Ref. 11 — to an open, dissipative system. Then for a generalized graphene band structure, both gapless and gapped (e.g., Sb-doped bismuth), we show how the susceptibility can be controlled using the bath. A wide-band bath with a nonzero LDOS over the bandwidth, introduces uniform decoherence and quenches the susceptibility for strong system-bath coupling. However, with engineered semiconducting and half-filled narrow bandwidth baths, which introduce non-uniform decoherence over the energy domain, we show that the susceptibility can be enhanced by increasing the system-bath coupling and can also be converted from paramagnetic to diamagnetic and vice versa. Furthermore we find that van Hove singularities in the bath LDOS can lead to giant enhancements in the susceptibility.

General multi-band model.–We begin with a general, multi-band electron Hamiltonian $H_S = \sum_{\mathbf{k}} \sum_{mn} \hat{\mathcal{H}}^{mn}_{\mathbf{k}} c^\dagger_{\mathbf{k}m} c_{\mathbf{k}n}$, where $c^\dagger_{\mathbf{k}m}$ ($c_{\mathbf{k}n}$) creates (annihilates) an electron with crystal momentum $\mathbf{k} = (k_x, k_y)$ in band m (n), and the band indices take the values $m, n = 1, 2, \ldots, \mathcal{N}$ [31]. The system is tunnel-coupled to a fermion bath, which is assumed to be equilibrated with temperature T and chemical potential μ. We fix the temperature to zero; however, the main results of this work should qualitatively hold at any finite low T, which should merely lead to trivial thermal broadening. Ignoring feedback effects of the system on the bath, the (inverse) retarded GF for the system in the presence of the bath can be written as $[\hat{g}_{\mathbf{k}}(\omega)]^{-1} = \omega - \hat{\mathcal{H}}_{\mathbf{k}}/\hbar - \hat{\Sigma}^R_{\mathbf{k}}(\omega)$, where $\hat{\Sigma}^R_{\mathbf{k}}(\omega)$ defines the retarded self-energy matrix arising due to system-bath coupling.

Since the real part of the self-energy does not play an essential role in the following discussion, we will ignore it and write $\hat{\Sigma}^R_{\mathbf{k}}(\omega) = -i\hat{\Gamma}_{\mathbf{k}}(\omega)$. Within the local tunneling approximation for the system-bath coupling, the retarded self-energy matrix becomes diagonal in band-space $\hat{\Gamma}_{\mathbf{k}}(\omega) = \Gamma(\omega) \equiv \pi\rho_B(\omega)|\xi|^2/\hbar$, where $\rho_B(\omega)$ is the LDOS of the bath, and ξ is the amplitude for system-bath tunneling [32]. Here, $\Gamma(\omega)$

measures the rate at which electrons with energy $\hbar\omega$ escape into the bath and introduces spectral broadening and decoherence to the band electrons [33].

Orbital magnetic susceptibility.–The gauge-invariant GF formalism developed by Onoda *et al*. [34] provides a general framework for systematically calculating the linear (and nonlinear) response of a band electron system to a uniform, static electromagnetic field. In a uniform, static magnetic field applied perpendicular to the system, i.e., $\mathbf{B} = B\hat{\mathbf{z}}$, the formalism leads to the following retarded GF up to second order in B,

$$\hat{G}_{\mathbf{k}}(\omega, B) = \hat{g}_{\mathbf{k}}(\omega) + i\left(\frac{eB}{2\hbar}\right)\hat{g}^{(1)}_{\mathbf{k}}(\omega) + \left(\frac{eB}{2\hbar}\right)^2 \hat{g}^{(2)}_{\mathbf{k}}(\omega)\,, \qquad (1)$$

where $(\omega, \mathbf{k})$ is now the mechanical energy-momentum vector, and the detailed expressions for $\hat{g}^{(1)}_{\mathbf{k}}(\omega)$ and $\hat{g}^{(2)}_{\mathbf{k}}(\omega)$ are provided in the Supplemental Material [32]. In the absence of the bath, Eq. (1) correctly reproduces the GF expression up to second order in B obtained recently using a different, gauge-invariant approach [11]. The orbital magnetic susceptibility of the dissipative, multi-band electron system is then given by

$$\chi = \frac{\mu_0 e^2}{S\hbar^2}\int\frac{d\omega}{2\pi}\,\Theta(\mu-\hbar\omega) \times\sum_{\mathbf{k}}\mathrm{Im}\left\{[\hbar(\omega+i\Gamma(\omega))-\mu]\,\mathrm{Tr}\left[\hat{g}^{(2)}_{\mathbf{k}}(\omega)\right]\right\}, \qquad (2)$$

where μ_0 is the vacuum permeability, S is the area of the 2D electron system, and $\Theta(x)$ is the Heaviside step function [32]. Equation (2) may be interpreted as the generalization of the result obtained recently [11] for a closed, multi-band electron system to the open, dissipative case. The difference between these two cases stems from the (energy-dependent) broadening of the electron levels $\Gamma(\omega)$, which modifies the electron density of states — the Tr term in Eq. (2) — as well as the energy prefactor $\hbar(\omega + i\Gamma(\omega))$. The controllability of χ is rooted in this energy-dependent level broadening.

Particle-hole symmetric two-band systems.–Let us apply Eq. (2) to a particle-hole symmetric, two-band system. Its Hamiltonian can be written generally as $\hat{\mathcal{H}}_{\mathbf{k}} = \mathbf{f}_{\mathbf{k}}\cdot\hat{\boldsymbol{\sigma}}$, where $\hat{\boldsymbol{\sigma}}$ is the vector of Pauli matrices in the sub-lattice space and $\mathbf{f}_{\mathbf{k}} = (f^x_{\mathbf{k}}, f^y_{\mathbf{k}}, f^z_{\mathbf{k}})$. The energy eigenvalues are $\pm\varepsilon_{\mathbf{k}}$, where $\varepsilon_{\mathbf{k}} = |\mathbf{f}_{\mathbf{k}}|$, and the energy eigenstates are characterized by the Berry curvature $\Omega_{ij}(\mathbf{k}) = -\mathbf{n}_{\mathbf{k}}\cdot(\mathbf{n}^i_{\mathbf{k}}\times\mathbf{n}^j_{\mathbf{k}})/2$, where $\mathbf{n}_{\mathbf{k}} = \mathbf{f}_{\mathbf{k}}/\varepsilon_{\mathbf{k}}$ and $\mathbf{n}^i_{\mathbf{k}} = \partial_{k_i}\mathbf{n}_{\mathbf{k}}$, and by the contra-variant geometric tensor

$$\begin{pmatrix} M^{xx} & M^{xy} \\ M^{yx} & M^{yy}\end{pmatrix} = \frac{1}{4}\begin{pmatrix} \mathbf{n}^y\cdot\mathbf{n}^y & -\mathbf{n}^x\cdot\mathbf{n}^y \\ -\mathbf{n}^x\cdot\mathbf{n}^y & \mathbf{n}^x\cdot\mathbf{n}^x\end{pmatrix}. \qquad (3)$$

The susceptibility Eq. (2) then become $\chi = \chi_{\mathrm{LP}} + \chi_\Omega + \chi_M$, where the first term is the intra-band Landau-Peierls term [1, 2], and the remaining two terms give the inter-band Berry curvature and geometric tensor contributions [11, 32, 35].

Defining the zero-field, retarded GF in the eigenbasis (labeled by $\alpha = \pm 1$) as $g^{-1}_{\mathbf{k}\alpha}(\omega) = \omega - \alpha\varepsilon_{\mathbf{k}}/\hbar + i\Gamma(\omega)$, the components of the susceptibility read

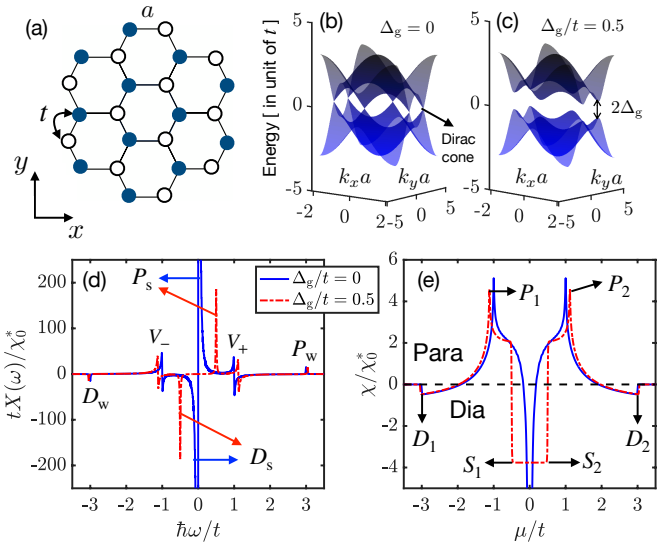


FIG. 1. (a) A schematic of the honeycomb lattice, where a and t are the lattice constant and the hopping amplitude, respectively. (b) and (c) are the band dispersions for the gapless and gapped graphene systems, respectively. (d) The susceptibility spectral function $X(\omega)$ for the closed system, i.e., $\Gamma(\omega) \to 0^+$. (e) The corresponding orbital susceptibility $\chi(\mu)$ [see Eq. (8)]. The spectral function $X(\omega)$ in (d) features a weak diamagnetic (paramagnetic) peak D_w (P_w), a strong diamagnetic (paramagnetic) peak D_s (P_s), and "double-peaks" $V_\pm$ due to the van Hove singularities in the electronic density of states. The corresponding $\chi(\mu)$ in (e) features weak diamagnetic kink ($D_{1/2}$) and strong paramagnetic peak ($P_{1/2}$). For gapless graphene the $\chi(\mu)$ also features a strong orbital diamagnetic peak at $\mu = 0$. Furthermore, the $\chi(\mu)$ of gapped graphene exhibits strong in-gap orbital diamagnetism between S_1 and S_2, where $-\Delta_g \le \mu \le \Delta_g$.

$$\chi_{\mathrm{LP}} = -\frac{\mu_0 e^2}{12\pi S\hbar^3}\int d\omega\sum_{\mathbf{k}\alpha}\mathrm{Im}\left[F(\omega)g^2_\alpha\right](\varepsilon_{xx}\varepsilon_{yy}-\varepsilon^2_{xy})\,, \qquad (4)$$

$$\chi_\Omega = -\frac{\mu_0 e^2}{\pi S\hbar^3}\int d\omega\sum_{\mathbf{k}\alpha}\mathrm{Im}\left[F(\omega)\left(\alpha\frac{\hbar g_\alpha}{\varepsilon}-g^2_\alpha\right)\right]\varepsilon^2\Omega^2_{xy}\,, \qquad (5)$$

$$\chi_M = -\frac{\mu_0 e^2}{\pi S\hbar^3}\int d\omega\sum_{\mathbf{k}\alpha}\mathrm{Im}\left[F(\omega)\left(\alpha\frac{\hbar g_\alpha}{\varepsilon}-g^2_\alpha\right)\right]\varepsilon_i\varepsilon_j M^{ij} + \frac{\mu_0 e^2}{2\pi S\hbar^3}\int d\omega\sum_{\mathbf{k}\alpha}\mathrm{Im}\left[F(\omega)\left(\alpha\frac{\hbar g_\alpha}{\varepsilon}\right)\right]\partial_{ij}\left(\varepsilon^2 M^{ij}\right), \qquad (6)$$

where we have suppressed the $(\omega, \mathbf{k})$ dependences for brevity, $\varepsilon_i = \partial_{k_i}\varepsilon_{\mathbf{k}}$, and $\varepsilon_{ij} = \partial_{k_i}\partial_{k_j}\varepsilon_{\mathbf{k}}$. The repeated indices in Eq. (6) are summed over with the understanding that $\partial_{ij} = \partial_{k_i}\partial_{k_j}$. In Eqs. (4)-(6), we have

$$F(\omega) = \frac{\partial}{\partial\omega}\left[\frac{\Theta(\mu/\hbar-\omega)\,(\omega-\mu/\hbar+i\Gamma(\omega))}{1+i\Gamma'(\omega)}\right], \qquad (7)$$

where $\Gamma'(\omega) = \partial\Gamma(\omega)/\partial\omega$. We here note that in the zero dissipation limit and in the absence of inter-band coupling, we can recover the Landau-Peierls formula of orbital magnetic susceptibility.

We now apply this result to a generalized graphene band structure, where $f^x_{\mathbf{k}} = t\cos(k_x a)+2t\cos(k_x a/2)\cos(\sqrt{3}k_y a/2)$, $f^y_{\mathbf{k}} = -t\sin(k_x a) + 2t\sin(k_x a/2)\cos(\sqrt{3}k_y a/2)$, and $f^z_{\mathbf{k}} = \Delta_g$ [32]. Here, $t > 0$ is the nearest-neighbor hopping amplitude on the honeycomb lattice and a is the distance between nearest-neighbor atoms [see Fig. 1(a)]; the band gap is $2\Delta_g$. Figures 1(b) and (c) show the energy dispersions for the gapless case ($\Delta_g = 0$) and a gapped case ($2\Delta_g = t$), respectively. Hereafter, χ is plotted in units of $\chi^*_0 = \mu_0 e^2 a^2 t/(12\pi\hbar^2)$.

Bath engineering.–To qualitatively illustrate how the susceptibility can be bath engineered, we first note that it can generally be expressed as the integral

$$\chi(\mu) = \hbar \int_{-\infty}^{\infty} d\omega\, \Theta(\mu - \hbar\omega) X(\omega)\,, \tag{8}$$

where we refer to $X(\omega)$ as the *susceptibility spectral function*. A plot of the spectral function for the generalized graphene system in the absence of the bath, i.e., $\Gamma(\omega) \to 0^+$, is shown in Fig. 1(d), where the solid blue (dashed red) curve corresponds to the gapless $\Delta_g = 0$ (gapped $2\Delta_g = t$) case [36]. The function features a weak diamagnetic (paramagnetic) peak $D_{\rm w}$ ($P_{\rm w}$), a strong diamagnetic (paramagnetic) peak $D_{\rm s}$ ($P_{\rm s}$), and "double-peaks" $V_\pm$ due to the van Hove singularities in the electronic density of states. The corresponding susceptibilities are given by the areas under $X(\omega)$ between $-\infty < \omega \le \mu/\hbar$ and are plotted in Fig. 1(e). In the figure, orbital paramagnetism for certain μ appears due to magnetic field-mediated inter-band coupling [5, 11].

We now open the system to the bath. If the bath LDOS is nonzero and constant over the entire bandwidth of the graphene system, the dissipation rate may be written $\Gamma(\omega) = \Gamma_{\rm b}$. In this case, increasing $\Gamma_{\rm b}$ broadens and washes out the sharp features in $X(\omega)$ over all energies and results in the vanishing of the χ for sufficiently strong $\Gamma_{\rm b}$ [32]. The latter appears to be consistent with the Bohr-van Leeuwen theorem.

With an ω-dependent dissipation rate $\Gamma(\omega)$, however, decoherence can be introduced to the electrons at selected energies. Therefore, a bath with non-trivial LDOS can be used to quench the coherent cyclotron orbits at certain frequencies while leaving those at other frequencies unaffected. We may go back to Fig. 1(d) and, for example, consider a bath with a robust LDOS at energies $\hbar\omega \ge 0$ and with zero LDOS for $\hbar\omega < 0$. Such a bath is expected to diminish the susceptibility spectral weight at $\hbar\omega \ge 0$, leading to the quenching of the peaks at $P_{\rm s}$, V_+, and $P_{\rm w}$, and to leave the peaks at $D_{\rm s}$, V_-, and $D_{\rm w}$ undisturbed. With such a bath, since $\chi(\mu)$ is given by the integral of the spectral function over $-\infty < \hbar\omega \le \mu$, one may be able to suppress the strong paramagnetic response at $\mu \approx t$ and may even turn the response diamagnetic. By selectively quenching the cyclotron orbits at certain energies, one can therefore try to engineer a desired orbital magnetic response as a function of μ. In what follows, we discuss the control of $\chi(\mu)$ for the generalized graphene system using two representative bath types: a semiconductor (SM) bath and a half-filled narrow bandwidth (NB) bath. We emphasize that the applicability of the idea of bath engineering is not limited to these two bath types. A new bath with a different LDOS can be used to induce a desired $\chi(\mu)$.

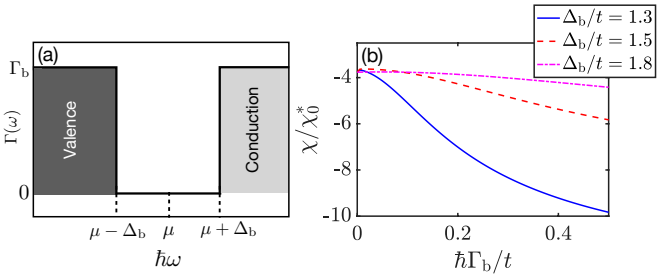


FIG. 2. (a) Dissipation rate $\Gamma(\omega)$ for a semiconducting bath. The gap between the valence (dark shaded) and the conduction (light shaded) bands is $2\Delta_{\rm b}$; the chemical potential μ is set at the center of the band gap. (b) χ vs. $\Gamma_{\rm b}$ for a gapped graphene system attached to the semiconducting bath: $\Delta_g = t/2$ and $\mu = 0$ are used.

Semiconducting bath.–The SM bath features a finite gap $2\Delta_{\rm b}$ between the valence and the conduction bands, and μ is located at the center of the band gap [see Fig. 2(a)]. The (ω-dispersive) dissipation rate here can be modeled by $\Gamma(\omega) = \Gamma_{\rm b}[\Theta(\mu - \Delta_{\rm b} - \hbar\omega) + \Theta(\hbar\omega - \mu - \Delta_{\rm b})]$, where $\Gamma_{\rm b}$ is the strength of dissipation. We discuss how this SM bath can enhance the in-gap diamagnetism of the gapped graphene system.

We fix the chemical potential of the bath (and of the system) to $\mu = 0$. In the absence of the bath, the system at the particle-hole symmetric point is diamagnetic [see Fig. 1(e)], owing to the strong diamagnetic spectral weight $D_{\rm s}$ [see Fig. 1(d)]. However, as per Eq. (8), $\chi(\mu = 0)$ is determined by the integral of $X(\omega)$ over $-\infty < \hbar\omega \le 0$, which consists of peaks $D_{\rm w}$, V_-, and $D_{\rm s}$. Though it may not be apparent from Fig. 1(d), the spectral weight in the region between $D_{\rm w}$ and V_- is slightly paramagnetic, which, when integrated over, leads to the gradual rise in paramagnetism — see the rise in the dashed red line in Fig. 1(e) from D_1 to P_1 — and to the strong paramagnetic peak P_1. We now place the valence band edge of the SM bath, i.e., $\mu - \Delta_{\rm b}$, somewhere in between the weak diamagnetic peak $D_{\rm w}$ and the van Hove point V_-. Such an SM bath "filters out" the paramagnetic spectral weight between $D_{\rm w}$ and $\mu - \Delta_{\rm b}$ while leaving the peak $D_{\rm s}$ undisturbed.

Integrating the filtered spectral function, we find that the diamagnetic susceptibility is enhanced as $\Gamma_{\rm b}$ is increased. This is shown in Fig. 2(b), which shows that the enhancement is most pronounced when the valence band edge of the SM bath is located at $-1.3t$ because the largest amount of paramagnetic spectral weight is filtered out in this case. Similar diamagnetic enhancement can be achieved as long as the center of the SM band gap is within the band gap of the gapped graphene and the bath valence band edge is set in between $D_{\rm w}$ and V_-.

Half-filled narrow bandwidth bath.–The half-filled NB bath features a nonzero LDOS over a finite bandwidth $2\Delta_{\rm bw}$, and μ is located at the center of the bandwidth [see Fig. 3(a)]. The dissipation rate here can be modeled by $\Gamma(\omega) = \Gamma_{\rm b}[1 - \Theta(\mu - \Delta_{\rm bw} - \hbar\omega) - \Theta(\hbar\omega - \mu - \Delta_{\rm bw})]$. We now show that a paramagnetic response of a gapped graphene system can be converted into a diamagnetic one using the half-filled NB bath.

The chemical potential of the bath (and of the system) is set to $\mu = t$, above the system's band gap. In the absence of the bath, the system at $\mu = t$ is paramagnetic, owing to the strong

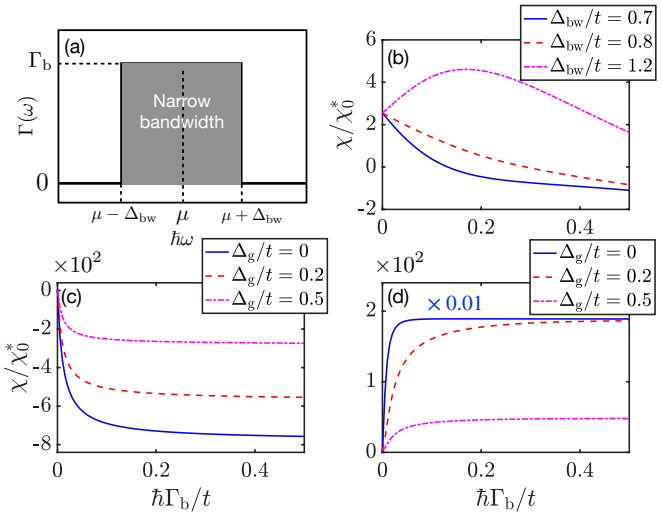


FIG. 3. (a) Dissipation rate $\Gamma(\omega)$ for a half-filled narrow bandwidth bath. The bandwidth is $2\Delta_{bw}$, and μ is set at the center of the band. (b)-(d) χ vs. Γ_b for the generalized graphene attached to the half-filled narrow bandwidth bath system with $\mu = t$: (b) is obtained for the gapped case $2\Delta_g = t$; (c) and (d) are obtained by aligning the lower band edge $\mu - \Delta_{bw}$ with the strong diamagnetic peak D_s and the strong paramagnetic peak P_s, respectively. For the gapless case $\Delta_g = 0$, (c) and (d) are obtained by placing the edge just slightly to the left and to the right of the charge neutrality point, respectively.

paramagnetic peak P_s [see Figs. 1(d) and (e)]. Once again, $\chi(\mu)$ is determined by the integral of $X(\omega)$ over $-\infty < \hbar\omega \leq t$, which consists of peaks D_w, V_-, D_s, and P_s. If the bottom of the bath band, i.e., $\mu - \Delta_{bw}$, is placed in between the strong diamagnetic peak D_s and the strong paramagnetic peak P_s, the NB bath can filter out the spectral weight over the energy interval $\mu - \Delta_{bw} \leq \hbar\omega \leq \mu$, including the P_s peak, while leaving the rest of the spectrum, including the D_s peak, undisturbed. This drives the paramagnetic response of the system at $\mu = t$ toward a diamagnetic one as Γ_b is increased.

This is illustrated by the solid blue and the dashed red curves in Fig. 3(b), which shows the paramagnetic-to-diamagnetic crossover with increasing Γ_b with the bottom of the bath band set at $0.3t$ and $0.2t$, respectively. Similar kind of paramagnetic-to-diamagnetic crossover can be achieved as long as $\mu - \Delta_{bw}$ is set between D_s and P_s and the chemical potential satisfies $\Delta_g < \mu \leq t$. The general tendency for the system to turn diamagnetic is observed also for the lower band edge at $\mu - \Delta_{bw} = -0.2t$, although for this case, the response is non-monotonic, where the system first becomes more paramagnetic before tending toward diamagnetism.

Van Hove Singularities.–The non-monotonic behavior seen in Fig. 3(b) for $\Delta_{bw}/t = 1.2$ cannot be explained solely by the bath-mediated spectral filtering and is rooted in the van Hove singularities of the bath LDOS. The NB bath features two van Hove singularities at $\hbar\omega_\pm = \mu \pm \Delta_{bw}$, where the derivatives of $\Gamma(\omega)$ are ill-defined, and these singularities play an important role in determining $\chi(\mu)$ via Eqs. (7) and (8). The van Hove singularity relevant for calculating $\chi(\mu)$ is at ω_-. When $\Delta_{bw}/t = 0.7$, ω_- is situated in between $\omega = 0$ and the paramagnetic peak P_s. The spectral weight in this region is weakly paramagnetic [see Fig. 1(d)], and when ω_- is in this region, it gives a strong diamagnetic contribution to χ. This is seen as the initial downturn in the χ vs. Γ_b curve seen for $\Delta_{bw}/t = 0.7$. For $\Delta_{bw}/t = 1.2$, ω_- is located in between the diamagnetic peak D_s and $\omega = 0$, where the spectral weight is weakly diamagnetic. The contribution to χ coming from the van Hove point then switches sign and becomes strongly paramagnetic. This leads to the initial upturn in the χ vs. Γ_b curve. All curves in Fig. 3(b) tend eventually toward diamagnetism due to spectral filtering, as discussed previously.

Interestingly, the van Hove singularities can be used to strongly enhance χ. To illustrate this, we again consider the half-filled NB bath and fix $\mu = t$. Giant enhancements in the χ are shown in Figs. 3(c) and (d) for three different gap sizes $\Delta_g = 0, 0.2t, 0.5t$. To obtain Figs. 3(c) and (d), the van Hove singularity ω_- of the half-filled NB bath was aligned with the strong diamagnetic peak D_s and the strong paramagnetic peak P_s, respectively, which are located at $\pm\Delta_g$. For $\Delta_g = 0$, Figs. 3(c) and (d) are obtained by placing ω_- just slightly to the left and to the right of the charge neutrality point, respectively. The van Hove singularity is marked by diverging derivatives of $\Gamma(\omega)$. We find that when such a singularity is brought in resonance with sharp features in the susceptibility spectral function — e.g., the D_s and P_s peaks — χ can exhibit a giant enhancement. When ω_- is brought in resonance with the P_s peak, we see a giant paramagnetic enhancement, while resonance with the D_s peak leads to a sign change in the susceptibility and to a giant diamagnetic enhancement. Within the current model, Figs. 3(c) and (d) show that the susceptibility can be enhanced by two orders of magnitude, and in the case of $\Delta_g = 0$ in Fig. 3(d), by four orders of magnitude. These giant enhancements cannot be explained solely in terms of spectral filtering discussed previously.

Conclusion.–In this work, we theoretically analyze how the orbital magnetic susceptibility of a 2D band electron system in a perpendicular magnetic field can be controlled by a dissipative bath. A suitably-tailored bath can be used to quench the coherent cyclotron motion of the electrons at certain energies while leaving those at other energies undisturbed. Moreover, van Hove singularities in the bath density of states can also selectively amplify the orbital response of electrons whose energies are in resonance with the singularities. These bath-induced effects, together with the fact that orbital magnetism in conductors is a Fermi sea phenomenon, are at the root of how the orbital magnetic response of band electrons can be manipulated with the bath. The LDOS used in this work is idealized to illustrate the concept of bath engineering as clearly as possible; however, as a future outlook, a more realistic LDOS should be considered to quantify the susceptibility with dissipation more precisely. Also, while this work discusses how bath engineering can be used to control the orbital magnetic response of an open band electron system, it is interesting to extend this idea to control other physical properties, where electrons from the entire Fermi sea contribute to the response: This may open wider range of applications in condensed matter physics, optomechanics and in the field of open quantum systems.

We acknowledge support by CUNY Research Foundation Project #90922-07 10. S. T. acknowledges PSC-CUNY Research Award Program #63515-00 51 and NSF CAREER Award DMR-2238135. S. C. acknowledges Universität Konstanz for providing necessary research facilities.

[1] L. Landau, Diamagnetismus der metalle, Zeitschrift für Physik **64**, 629 (1930).
[2] R. Peierls, Zur theorie des diamagnetismus von leitungselektronen, Zeitschrift für Physik **80**, 763 (1933).
[3] P. R. Wallace, The band theory of graphite, Phys. Rev. **71**, 622 (1947).
[4] J. W. McClure, Diamagnetism of graphite, Phys. Rev. **104**, 666 (1956).
[5] G. Vignale, Orbital paramagnetism of electrons in a two-dimensional lattice, Phys. Rev. Lett. **67**, 358 (1991).
[6] H. Fukuyama and R. Kubo, Interband effects on magnetic susceptibility. ii. diamagnetism of bismuth, J. Phys. Soc. Jpn **28**, 570 (1970).
[7] H. Fukuyama, Theory of Orbital Magnetism of Bloch Electrons: Coulomb Interactions, Prog. Theor. Phys. **45**, 704 (1971).
[8] H. Fukuyama, Anomalous orbital magnetism and hall effect of massless fermions in two dimension, Journal of the Physical Society of Japan **76**, 043711 (2007), https://doi.org/10.1143/JPSJ.76.043711.
[9] M. Koshino and T. Ando, Orbital diamagnetism in multilayer graphenes: Systematic study with the effective mass approximation, Phys. Rev. B **76**, 085425 (2007).
[10] G. Gómez-Santos and T. Stauber, Measurable lattice effects on the charge and magnetic response in graphene, Phys. Rev. Lett. **106**, 045504 (2011).
[11] A. Raoux, F. Piéchon, J.-N. Fuchs, and G. Montambaux, Orbital magnetism in coupled-bands models, Phys. Rev. B **91**, 085120 (2015).
[12] Y. Ominato and M. Koshino, Orbital magnetism of graphene flakes, Phys. Rev. B **87**, 115433 (2013).
[13] Z. Li, L. Chen, S. Meng, L. Guo, J. Huang, Y. Liu, W. Wang, and X. Chen, Field and temperature dependence of intrinsic diamagnetism in graphene: Theory and experiment, Phys. Rev. B **91**, 094429 (2015).
[14] S. Suetsugu, K. Kitagawa, T. Kariyado, A. W. Rost, J. Nuss, C. Mühle, M. Ogata, and H. Takagi, Giant orbital diamagnetism of three-dimensional dirac electrons in sr_3PbO antiperovskite, Phys. Rev. B **103**, 115117 (2021).
[15] J. Vallejo Bustamante, *Singular orbital diamagnetism and paramagnetism in graphene*, Theses, Université Paris-Saclay (2023).
[16] G. A. H. Schober, H. Murakawa, M. S. Bahramy, R. Arita, Y. Kaneko, Y. Tokura, and N. Nagaosa, Mechanisms of enhanced orbital dia- and paramagnetism: Application to the rashba semiconductor bitei, Phys. Rev. Lett. **108**, 247208 (2012).
[17] H. Suzuura and T. Ando, Theory of magnetic response in two-dimensional giant rashba system, Phys. Rev. B **94**, 085303 (2016).
[18] M. S. Bahramy and N. Ogawa, Bulk rashba semiconductors and related quantum phenomena, Advanced Materials **29**, 1605911 (2017).
[19] N. Bohr, *Studier over Metallernes Elektrontheori*, Ph.D. thesis, University of Copenhagen (1911).
[20] H. J. van Leeuwen, Problèmes de la théorie électronique du magnétisme, J. Phys. Radium **2**, 361 (1921).
[21] J. H. Van Vleck, *The Theory of Electric and Magnetic Susceptibilities* (Oxford University Press, London, 1932).
[22] A. Caldeira and A. Leggett, Quantum tunnelling in a dissipative system, Ann. Phys. **149**, 374 (1983).
[23] K. Lindenberg and B. J. West, *The Nonequilibrium Statistical Mechanics of Open and Closed* (VCH, New York, 1990).
[24] N. G. van Kampen, *Stochastic Processes in Physics and Chemistry* (Elsevier Science, Amsterdam, 2007).
[25] Y. Marathe, Dissipative quantum dynamics of a charged particle in a magnetic field, Phys. Rev. A **39**, 5927 (1989).
[26] X. L. Li, G. W. Ford, and R. F. O'Connell, Magnetic-field effects on the motion of a charged particle in a heat bath, Phys. Rev. A **41**, 5287 (1990).
[27] S. Dattagupta and J. Singh, Landau diamagnetism in a dissipative and confined system, Phys. Rev. Lett. **79**, 961 (1997).
[28] M. Bandyopadhyay and S. Dattagupta, Landau–drude diamagnetism: fluctuation, dissipation and decoherence, J. Phys.: Condens. Matter **18**, 10029 (2006).
[29] U. Satpathi and S. Sinha, Non-equilibrium quantum langevin dynamics of orbital diamagnetic moment, J. Stat. Phys. **2019**, 063106 (2019).
[30] E. K. Alpomishev, G. G. Adamian, and N. V. Antonenko, Orbital diamagnetism of two-dimensional quantum systems in a dissipative environment: Non-markovian effect and application to graphene, Phys. Rev. E **104**, 054120 (2021).
[31] In this work, we consider spinless electrons and focus solely on orbital magnetism.
[32] See Supplemental Material.
[33] The introduction of the dissipative bath within the local tunneling approximation does not lead to couplings between the bands; however, our work can be readily generalized to the case where the bath also induces inter-band coupling.
[34] S. Onoda, N. Sugimoto, and N. Nagaosa, Theory of non-equilibirum states driven by constant electromagnetic fields, Prog. Theor. Phys. **116**, 61 (2006).
[35] F. Piéchon, A. Raoux, J.-N. Fuchs, and G. Montambaux, Geometric orbital susceptibility: Quantum metric without berry curvature, Phys. Rev. B **94**, 134423 (2016).
[36] The spectral function $X(\omega)$ obeys $X(-\omega) = -X(\omega)$ due to particle-hole symmetry.